further the interesting parallels between group 4 and group 14 organometallic chemistry.

Acknowledgment. W.E.P. thanks the Natural Sciences and Engineering Research Council of Canada for financial support of this work and Professor John D. Goddard for helpful discussions.

Supplementary Material Available: Tables containing full bond distance and angle data, anisotropic thermal parameters, hydrogen positional and thermal parameters, torsion angles, and mean plane data for **1b** (8 pages). Ordering information is given on any current masthead page.

OM920461W

Differential Reactivity of the Dihydrides $Mn_2(\mu\text{-}H)_2(CO)_6(\mu\text{-}L\text{-}L)$ (L-L = $(EtO)_2POP(OEt)_2$, $Ph_2PCH_2PPh_2$) toward $Fe_2(CO)_9$ or $M(CO)_6$ (M = Cr, Mo, W). X-ray Crystal Structure of $Mn_2Fe(\mu\text{-}H)(\mu\text{-}PhPCH_2PPh_2)(CO)_{10}$

Remedios Carreño, Víctor Riera,* and Miguel A. Ruiz

Departamento de Química Organometálica, Universidad de Oviedo, 33071 Oviedo, Spain

Claudette Bois and Yves Jeannin

Laboratoire de Chimie des Metaux de Transition, UA-CNRS 419, Université P. et M. Curie,
75252 Paris Cedex 05, France

Received May 11, 1992

Reaction of $Mn_2(\mu\text{-}H)_2(\mu\text{-}tedip)(CO)_6$ (tedip = $(EtO)_2POP(OEt)_2$) with $Fe_2(CO)_9$ at room temperature leads to $Mn_2Fe(\mu\text{-}H)_2(\mu\text{-}tedip)(CO)_{10}$, resulting from the insertion of a $Fe(CO)_4$ fragment into an $Mn_2(\mu\text{-}H)$ bond in the parent hydride. Two isomers of this cluster are present in solution. Both have the tedip ligand bridging Mn and Fe atoms and differ in the position of the hydrido ligands, as revealed by NMR data. Reaction of $Mn_2(\mu\text{-}H)_2(\mu\text{-}dppm)(CO)_6$ (dppm = $Ph_2PCH_2PPh_2$) with $Fe_2(CO)_9$ at room temperature occurs with benzene elimination to yield $Mn_2Fe(\mu\text{-}H)(\mu\text{-}PhPCH_2PPh_2)(CO)_{10}$, the structure of which has been determined by X-ray diffraction. The cluster crystallizes in the space group $P2_1/n$ (a = 9.887 (2) Å, b = 35.554 (4) Å, c = 9.682 (1) Å, β = 116.93 (2)°, V = 3034 (1) Å^3, Z = 4). The structure was refined to R = 0.0376 (R_w = 0.0370) for 4079 reflections with $I \geq 3\sigma(I)$. The cluster contains an Mn_2Fe triangle (Mn(1)–Fe = 2.9065 (5) Å, Mn(2)–Fe = 2.7247 (5) Å, Mn–Mn = 2.8917 (6) Å) triply bridged by the phosphido–phosphine ligand $PhPCH_2PPh_2$ and a hydrido ligand. Both the hydride and the phosphido group are over the Mn(2)–Fe edge. Each metal atom has three essentially linear carbonyl ligands. Mn(1) bears one carbonyl more, which has a semibridging interaction with Mn(2) (Mn(1)–C(7)–O(7) = 160.0 (3)°, Mn(1)–C(7) = 1.872 (3) Å, Mn(2)–C(7) = 2.521 (3) Å). Low-temperature UV irradiation of $Mn_2(\mu\text{-}H)_2(\mu\text{-}tedip)(CO)_6$ in the presence of $W(CO)_6$ leads to the thermally unstable cluster $Mn_2W(\mu_2\text{-}H)(\mu_3\text{-}H)(\mu\text{-}tedip)(CO)_{11}$, which can be isolated in high yield. The analogous molybdenum compound could not be isolated, but its formation could be detected by low-temperature NMR spectroscopy, which revealed the presence of two new species in solution. The formation and structures of the new clusters reported are discussed in light of the isolobal analogies.

Introduction

Wade rules[1] and the isolobal principle developed by Hoffman,[2] Mingos,[3] and others represent a powerful tool not only for a unified understanding of the electronic and physical structures of the organic, inorganic, or organometallic molecules but also for designing rational synthetic routes to specific compounds through the building-block approach. The latter has been particularly successful in the field of di- and polynuclear transition-metal carbonyls, of which the inspired work of Stone[4] is a relevant example.

We have already considered the isolobal relationship $H^+ \leftrightarrow AuPPh_3^+$ in our general study on the reactivity of the unsaturated dimanganese hydrides $Mn_2(\mu\text{-}H)_2(\mu\text{-}L\text{-}L)(CO)_6$ (**1**, L-L = $(EtO)_2POP(OEt)_2$, (tedip);[5] **2**, L-L = $Ph_2PCH_2PPh_2$ (dppm)[6]). This has led us to the synthesis of heterometallic unsaturated clusters such as $Mn_2(\mu\text{-}AuPPh_3)(\mu\text{-}H)(\mu\text{-}L\text{-}L)(CO)_6$ or the cationic $Mn_2(\mu\text{-}AuPPh_3)(\mu\text{-}H)_2(\mu\text{-}dppm)(CO)_6^+$.[7] The structure of the latter points to a Lewis-base behavior of the neutral precursor **2**, in marked contrast with the Lewis-acid behavior expected for this electron-deficient species, as shown by

---

[1] Wade, K. *Adv. Inorg. Chem. Radiochem.* **1976**, *18*, 1.

[2] Hoffmann, R. *Angew. Chem., Int. Ed. Engl.* **1982**, *21*, 711.

[3] Evans, D. G.; Mingos, D. M. P. *J. Organomet. Chem.* **1982**, *232*, 171.

[4] (a) Stone, F. G. A. *Angew. Chem., Int. Ed. Engl.* **1984**, *23*, 89. (b) Stone, F. G. A. *Adv. Organomet. Chem.* **1990**, *31*, 53. (c) For a recent paper see for example: Brew, S. A.; Carr, N.; Mortimer, M. D.; Stone, F. G. A. *J. Chem. Soc., Dalton Trans.* **1991**, 811 and references therein.

[5] Riera, V.; Ruiz, M. A.; Tiripicchio, A.; Tiripicchio-Camellini, M. *J. Chem. Soc., Chem. Commun.* **1985**, 1505.

[6] (a) García Alonso, F. J.; García-Sanz, M.; Riera, V.; Ruiz, M. A.; Tiripicchio, A.; Tiripicchio-Camellini, M. *Angew. Chem., Int. Ed. Engl.* **1988**, *27*, 1167. (b) García Alonso, F. J.; Riera, V.; Ruiz, M. A.; Tiripicchio, A.; Tiripicchio-Camellini, M. *Organometallics* **1992**, *11*, 370.

[7] Carreño, R.; Riera, V.; Ruiz, M. A.; Bois, C.; Jeannin, Y. *Organometallics* **1992**, *11*, 2923.

0276-7333/92/2311-4022$03.00/0

Table I. NMR Data for New Compounds

compd	^{1}H NMR/δ^a	^{31}P{^{1}H} NMR/δ^a
$Mn_2Fe(\mu\text{-}H)_2(\mu\text{-tedip})(CO)_{10}$ (**3**)		
isomer **3a**	4.2–3.7 (m, CH_2); 1.34, 1.33, 1.30, 1.26 (4 × t, 7,^{b} CH_3); −16.9 [d, 21,^{c} Mn(μ-H)Mn]; −20.7 [dd, 25,^{c} 37,^{c} Fe(μ-H)Mn]	167.5 (br, P–Mn); 161.9 (d, 100,^{d} P–Fe) 168.9^e (d, 102,^{d} P–Mn); 164.4^e (d, P–Fe)
isomer **3b**	−19.6 [d, 15,^{c} Mn(μ-H)Mn]; −23.6 [s, Mn(μ-H)Fe]	168.5^e (d, 74,^{d} P–Mn); 161.5^e (d, P–Fe)
$Mn_2Fe(\mu\text{-}H)(\mu\text{-}Ph_2PCH_2PPh)(CO)_{10}$ (**4**)	7.6–7.0 (m, C_6H_5); 3.8–3.9 (m, CH_2); −15.2 [d, 27,^{c} Mn(μ-H)Fe]	157.2 (d, 100,^{d} μ-PPh); 39.8 (d, PPh_2)
$Mn_2W(\mu\text{-}H)_2(\mu\text{-tedip})(CO)_{11}{}^f$ (**5**)	4.2–4.1 (m, 3 × CH_2); 4.0–3.9 (m, 1 × CH_2); 1.3, 1.2 (2 × t, 7,^{b} CH_3); −17.1 (td, 27,^{c} 5,^{g} μ_2-H); −24.0 (td, 21,^{c} 5,^{g} μ_3-H)^h	163.3 (s, P–Mn)
$Mn_2Mo(\mu\text{-}H)_2(\mu\text{-tedip})(CO)_{11}{}^f$ (**6**)		
isomer **6a**	−17.3 (t, 29,^{c} μ_2-H); −25.0 (t, 23,^{c} μ_3-H)	164.0 (s, P–Mn)
isomer **6b**	−14.5 [d, 44,^{c} Mn(μ-H)Mo]; −24.1 [t, 29,^{c} Mn(μ-H)Mn]	173.4 (d, br, 50,^{d} P–Mn)^i

[a] Measured in CD_2Cl_2 at 295 K unless otherwise stated. Positive values correspond to frequencies higher than the reference. Coupling constants are given in Hz. [b] ^3J(HH). [c] J(PH). [d] J(PP). [e] 195 K. [f] 243 K. [g] ^2J(HH). [h] J(WH) = 40 Hz, at 273 K. [i] The other phosphorus resonance is probably hidden under that of compound 1 (see text).

the high reactivity of **1** or **2**, under mild conditions, toward a variety of potential electron donors such as phosphines,[8a] alkynes,[6b] carbon dioxide,[8c] and isocyanides or nitriles.[8b] We report here the reactions between the unsaturated hydrides **1** and **2** and either $Fe_2(CO)_9$ or $M(CO)_6$ (M = W, Mo, Cr), under conditions where the metal fragments "$Fe(CO)_4$" or "$M(CO)_5$" are expected to be formed. This should give us an indication of the utility of these reactions as synthetic routes to heterometallic clusters containing manganese and middle transition metals, of which there are few examples in the literature. On the other hand, as found for other metal fragments, the isolobal relationships are not a one-to-one mapping. In particular, the aforementioned $M(CO)_5$ and $M(CO)_4$ fragments can be considered isolobal either with CH_2 or with CH_3^+ (and then H^+).[2] For this reason, it was also of interest to examine in which way the electronic deficiency of **1** or **2** on the one hand, and that of the $Fe(CO)_4$ or $M(CO)_5$ metal fragments on the other, would determine the nature of the resulting interactions. Previous related work in this direction is scarce, it being essentially restricted to the reactions of $Os_3(\mu\text{-}H_2)(CO)_{10}$ (Os=Os) toward $Fe_2(CO)_9$[9] or $M(C_2H_4)L(PPh_3)$[10] (M = Ni, L = PPh_3; M = Pt, L = PPh_3, C_2H_4) and of $Re_2(\mu\text{-}H)_2(CO)_8$ (Re=Re) toward $Pt(C_2H_4)(PPh_3)_2$.[11,12] In all of these reactions, the behavior of the corresponding d^8 ML$_4$ or d^{10} ML$_2$ fragments can be interpreted as CH_2-like. In contrast with this, our results show that the $Fe(CO)_4$ and $M(CO)_5$ fragments display quite different behaviors when faced with each of the unsaturated hydrides **1** and **2**.

Table II. Experimental Data for the Crystallographic Analysis of $Mn_2Fe(\mu\text{-}H)(\mu\text{-}PhPCH_2PPh_2)(CO)_{10}$ (4)

formula	$C_{29}H_{18}FeMn_2O_{10}P_2$
mw	754.1
cryst syst	monoclinic
space group	$P2_1/n$
a, Å	9.887 (2)
b, Å	35.554 (4)
c, Å	9.682 (1)
β, deg	116.93 (2)
V, Å^3	3034 (1)
Z	4
ρ(calcd), g cm^{-3}	1.65
rflns for lattice params	
no.	25
range (θ), deg	16–17
F(000)	1512
temp, °C	18
cryst size, mm	0.60 × 0.55 × 0.40
diffractometer	Philips PW1100
monochromator	graphite
radiation	Mo Kα
scan mode	ω–2θ
scan width	0.80 + 0.345 tan θ
θ range, deg	1–25
std rflns	2, measd every 2 h
μ, cm^{-1}	14.2
no. of measd rflns	5083
no. of reflns used with $I \geq 3\sigma(I)$	4079
min, max final $\Delta\rho$, e Å^{-3}	−0.55, +0.60
no. of refined params	448
$R = [\sum\lvert\Delta F\rvert/\sum F_o]$	0.0376
$R_w = [\sum w(\Delta F)^2/\sum wF_o^2]^{1/2\,a}$	0.0370

[a] $w = 1/\sum_{r=1,3} A_r T_r(x)$, with three coefficients 1.93, 0.72, 1.54 for a Chebyshev series, for which $x = F_o/F_o(\max)$.

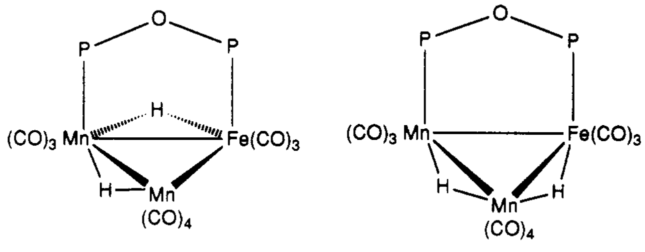

3a **3b**

Figure 1. Proposed structures for the isomers detected in compound 3 (POP = $(EtO)_2POP(OEt)_2$).

Results and Discussion

Reaction of 1 with $Fe_2(CO)_9$. Compound **1** reacts readily with stoichiometric amounts of $Fe_2(CO)_9$ in toluene at room temperature to afford the trimetallic dark red cluster $Mn_2Fe(\mu\text{-}H)_2(\mu\text{-tedip})(CO)_{10}$ (**3**) in high yield. No reaction was observed when tetrahydrofuran was used as solvent. This can be explained by assuming that **1** is not able to displace the tetrahydrofuran (thf) molecule in the complex $Fe(CO)_4$(thf). As is well-known, this labile species is formed when $Fe_2(CO)_9$ is stirred in tetrahydrofuran. Compound **3**, however, is stable in tetrahydrofuran solution, and therefore some irreversible structural rearrangement in the adduct **1**·$Fe(CO)_4$, presumably formed in a first step, can be expected.

The IR spectrum of **3** in petroleum ether solution shows seven bands. The band at 2081 cm^{-1} suggests the presence of an $M(CO)_4$ fragment in the molecule, since $M(CO)_3$ groups in this kind of compound generally give rise to

---

[8] (a) Carreño, R.; Riera, V.; Ruiz, M. A.; Bois, C.; Jeannin, Y. *J. Organomet. Chem.* **1991**, *419*, 163. (b) García Alonso, F. J.; García-Sanz, M.; Riera, V.; Tiripicchio, A.; Tiripicchio-Camellini, M. *Organometallics* **1992**, *11*, 801. (c) García Alonso, F. J.; García Sanz, M.; Riera, V. *J. Organomet. Chem.* **1991**, *421*, C12.

[9] Plotkin, J. S.; Alway, D. G.; Weisenberger, C. R.; Shore, S. G. *J. Am. Chem. Soc.* **1980**, *102*, 6157.

[10] (a) Farrugia, L. J.; Howard, J. A. K.; Mitrprachachon, P.; Spencer, F. L.; Stone, F. G. A.; Woodward, P. *J. Chem. Soc., Chem. Commun.* **1978**, 260. (b) Farrugia, L. J.; Howard, J. A. K.; Mitrprachachon, P.; Spencer, F. L.; Stone, F. G. A.; Woodward, P. *J. Chem. Soc., Dalton Trans.* **1981**, 155.

[11] Stone, F. G. A. *Acc. Chem. Res.* **1981**, *14*, 318.

[12] (a) Beringhelli, T.; Ceriotti, A.; D'Alfonso, G.; Della Pergola, R. *Organometallics* **1990**, *9*, 1053. (b) Beringhelli, T.; D'Alfonso, G.; Minoja, A. P. *Organometallics* **1991**, *10*, 394.

Table III. Atomic Coordinates and Thermal Parameters for Non-Hydrogen Atoms and the Hydrido Ligand in Compound 4

atom	*x*/*a*	*y*/*b*	*z*/*c*	*U*(equiv)
Fe(1)	0.21298 (4)	0.10863 (1)	0.54218 (5)	0.0330
Mn(1)	–0.09513 (5)	0.08278 (1)	0.44875 (5)	0.0327
Mn(2)	0.01025 (5)	0.15791 (1)	0.55967 (5)	0.0312
P(1)	0.07747 (8)	0.15199 (2)	0.36891 (8)	0.0308
P(2)	–0.18496 (8)	0.10295 (2)	0.19271 (8)	0.0336
O(1)	0.3371 (3)	0.05034 (7)	0.7857 (3)	0.0597
O(2)	0.4867 (3)	0.15371 (8)	0.7039 (3)	0.0646
O(3)	0.3071 (4)	0.7542 (8)	0.3233 (4)	0.0719
O(4)	0.0192 (3)	0.05935 (7)	0.7779 (3)	0.0527
O(5)	0.0773 (3)	0.02069 (6)	0.3939 (3)	0.0562
O(6)	–0.3496 (3)	0.03052 (8)	0.3699 (3)	0.0649
O(7)	–0.3289 (3)	0.12991 (7)	0.4802 (3)	0.0547
O(8)	–0.0205 (3)	0.15120 (8)	0.8485 (3)	0.0594
O(9)	0.2217 (3)	0.22122 (7)	0.6875 (3)	0.0634
O(10)	–0.2262 (3)	0.21564 (8)	0.4223 (3)	0.0641
C(1)	0.2875 (3)	0.07267 (9)	0.6927 (4)	0.0420
C(2)	0.3800 (3)	0.13651 (9)	0.6390 (4)	0.0443
C(3)	0.2692 (4)	0.08769 (9)	0.4083 (4)	0.0479
C(4)	–0.0216 (3)	0.06855 (9)	0.6535 (4)	0.0421
C(5)	0.0223 (4)	0.04652 (9)	0.4165 (3)	0.0427
C(6)	–0.2513 (4)	0.05048 (9)	0.3961 (4)	0.0444
C(7)	–0.2239 (3)	0.11765 (9)	0.4739 (3)	0.0423
C(8)	–0.0086 (3)	0.15306 (8)	0.7374 (3)	0.0408
C(9)	0.1401 (4)	0.19636 (9)	0.6393 (3)	0.0443
C(10)	–0.1388 (4)	0.19194 (9)	0.4711 (4)	0.0446
C(11)	–0.0456 (4)	0.13362 (9)	0.1744 (3)	0.0373
C(20)	0.1674 (3)	0.19239 (8)	0.3274 (3)	0.0369
C(21)	0.0861 (5)	0.2254 (1)	0.2798 (5)	0.0621
C(22)	0.1539 (8)	0.2570 (1)	0.2580 (7)	0.0810
C(23)	0.3003 (7)	0.2567 (1)	0.2844 (7)	0.0764
C(24)	0.3808 (6)	0.2243 (2)	0.3283 (6)	0.0714
C(25)	0.3161 (4)	0.1919 (1)	0.3503 (5)	0.0572
C(30)	–0.3587 (3)	0.13079 (9)	0.1213 (3)	0.0384
C(31)	–0.3654 (4)	0.1693 (1)	0.0968 (4)	0.0540
C(32)	–0.5010 (5)	0.1884 (1)	0.0487 (5)	0.0651
C(33)	–0.6300 (5)	0.1696 (1)	0.0245 (5)	0.0642
C(34)	–0.6271 (4)	0.1312 (1)	0.0469 (4)	0.0611
C(35)	–0.4922 (4)	0.1119 (1)	0.0948 (4)	0.0509
C(40)	–0.2350 (3)	0.06909 (9)	0.0349 (3)	0.0391
C(41)	–0.2752 (4)	0.0828 (1)	–0.1129 (4)	0.0446
C(42)	–0.3187 (4)	0.0583 (1)	–0.2367 (4)	0.0496
C(43)	–0.3218 (4)	0.0205 (1)	–0.2160 (4)	0.0568
C(44)	–0.2842 (6)	0.0065 (1)	–0.0710 (5)	0.0669
C(45)	–0.2399 (5)	0.0306 (1)	0.0546 (4)	0.0575
H(1)	0.154 (4)	0.124 (1)	0.655 (4)	0.071 (3)

absorptions below 2060 cm^{-1}. On the other hand, NMR data (Table I) indicate that compound **3** exists in solution as an unresolvable mixture of two isomers (**3a,b**; Figure 1) in a **3a**:**3b** ratio of ca. 8:1. This proportion was found to be essentially solvent and temperature independent. Solvents used were fully deuterated chloroform, dichloromethane, benzene, cyclohexane, toluene, and acetone (substantial decomposition occurred in the last solvent). The range of temperatures analyzed was +25 to −90 °C (dichloromethane or toluene solutions). Black crystals of **3** can be grown by crystallization from petroleum ether at −20 °C. Unfortunately, they were found unsuitable for X-ray diffraction. However, the NMR spectra recorded after dissolving one of these crystals showed the same **3a**:**3b** ratio described above. We explain this by assuming that **3a** and **3b** can interconvert so as to reach the equilibrium distribution rapidly on the laboratory time scale (seconds) but not fast enough on the NMR time scale. As a result, their resonances can be observed separately. This is further supported by the observation that the **3a**:**3b** ratio in solutions of **3** briefly exposed to the air (and therefore substantially decomposed) has the same value previously mentioned. However, the possibility that **3a** and **3b** do not interconvert, but rather cocrystallize, cannot be ruled out completely. This would, at least, require **3a** and **3b** to react with the atmospheric agents at the same rate.

Both **3a** and **3b** contain two nonequivalent hydrido ligands and phosphorus atoms. Moreover, the latter give rise in the ^{31}P NMR spectrum to a sharp doublet and a broad resonance. This indicates that one of the P atoms is coordinated to iron and the second one to manganese, the broadening effect being due to the ^{31}P–^{55}Mn scalar coupling. As expected, when the solution is cooled, the broad resonances sharpen, and broad doublets for P(Mn) atoms are observed at 195 K (Table I), for both **3a** and **3b**. The structure proposed for these isomers is derived from the structures found for $Mn_3(\mu\text{-}H)_3(CO)_{12}$[13] or $Re_3(\mu\text{-}H)_3(CO)_8(\mu\text{-tedip})_2$,[14] after replacement of an $HM(CO)_4$ moiety (M = Mn, Re) by the isoelectronic fragment $Fe(CO)_4$. The bridging tetraethyl pyrophosphite ligand is thought to be occupying positions on the metal atoms perpendicular to the metal triangle, as in the mentioned trirhenium species. The hydride resonances for the major isomer exhibit normal ^2J(PH) couplings either with one or with two phosphorus atoms and are thus assigned to $Mn(\mu\text{-}H)Mn$ and $Mn(\mu\text{-}H)Fe$ bridges, respectively (**3a** in Figure 1). The interpretation of the resonances for the minor isomer is less straightforward. They appear as a doublet at −19.63 ppm (*J*(PH) = 15 Hz) and a singlet at −23.6 ppm. The moderate broadness of the latter ($w_{1/2}$ = ca. 10 Hz) could be hiding a small coupling, but in any case this (or the coupling shown by the low-field resonance) must be considered as significantly low. We have previously found an unusually low ^2J(PH) value for the $Mn(\mu\text{-}H)Sn$ hydrido ligand in $Mn_2(\mu\text{-}H)(\mu\text{-}HSnPh_2)(\mu\text{-dppm})(CO)_6$,[15] closely related to **3** by considering the relationship $Fe(CO)_4/SnPh_2$. In the case of **3b**, this can be interpreted as an indication of a weak H–Fe interaction in the $Mn(\mu\text{-}H)Fe$ bridge. Indeed, in addition to the fact that both **3a** and **3b** are 48e clusters, and therefore electron precise, the hydrido ligands are expected to be located asymmetrically across the metal edges. This is deduced not only from symmetry considerations but also from the fact that an equal sharing of the hydride electron densities would render odd electron counts around the metals (18.5 electrons around iron, 18 and 17.5 electrons around the manganese atoms).

On the whole, if we ignore the exchange between CO and P positions, the reaction leading to complex **3** can be viewed as the insertion of an $Fe(CO)_4$ fragment into an Mn–H bond of the unsaturated moiety present in the dihydride **1**. This strongly resembles the reaction of the related dihydride $Os_3(\mu\text{-}H)_2(CO)_{10}$ (Os=Os) with CH_2N_2, which leads to the methyl complex $Os_3(\mu\text{-}H)(\mu\text{-}\eta^2\text{-}CH_3)(CO)_{10}$, in equilibrium with the methylene species $Os_3(\mu\text{-}H)_2(\mu\text{-}CH_2)(CO)_{10}$.[16] Thus, it can be concluded that the $Fe(CO)_4$ fragment behaves as CH_2 when faced with complex **1**. At present, we do not know the cause for the secondary process observed in this reaction, i.e., the coordination of one of the phosphorus atoms of the tedip ligand to iron, compensated by the transfer of one CO ligand from iron to manganese. It should be pointed out that an analogous P/CO exchange occurs in the reaction of $Re_2(\mu\text{-}H)_2(CO)_8$ with $Pt(C_2H_4)(PPh_3)_2$,[11,12] where one

---

[13] Kirtley, S. W.; Olsen, J. P.; Bau, R. *J. Am. Chem. Soc.* **1973**, *95*, 4532.

[14] Prest, D. W.; Mays, M. J.; Raithby, P. R.; Orpen, A. G. *J. Chem. Soc., Dalton Trans.* **1982**, 737.

[15] Carreño, R.; Riera, V.; Ruiz, M. A.; Bois, C.; Jeannin, Y. *J. Chem. Soc., Chem. Commun.* **1990**, 15.

[16] (a) Calvert, R. B.; Shapley, J. R.; Williams, J. M.; Suib, S. L.; Stucky, G. D. *J. Am. Chem. Soc.* **1978**, *100*, 6240. (b) Calvert, R. B.; Shapley, J. R. *J. Am. Chem. Soc.* **1977**, *99*, 5225; **1978**, *100*, 7726. (c) Schultz, A. J.; Williams, J. M.; Calvert, R. B.; Shapley, J. R.; Stucky, G. D. *Inorg. Chem.* **1979**, *18*, 319.

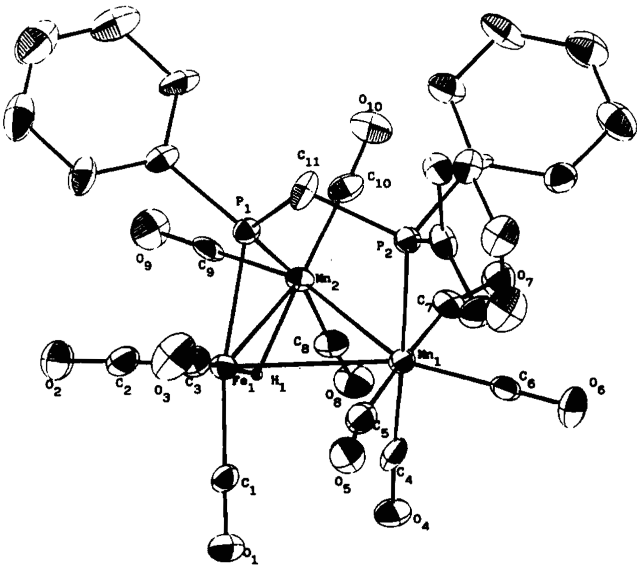

Figure 2. ORTEP drawing of the molecular structure of $[Mn_2Fe(\mu\text{-}H)(\mu\text{-}PhPCH_2PPh_2)(CO)_{10}]$ (4) (C(Ph) labels omitted for clarity).

PPh_3 ligand migrates from Pt to Re and one CO ligand is transferred from Re to Pt.

Reaction of 2 with $Fe_2(CO)_9$. The dppm-bridged dihydride 2 also reacts rapidly with $Fe_2(CO)_9$ in toluene even at 0 °C. In this case, surprisingly, benzene is eliminated (as confirmed by GC-MS from the reaction solution) and the new phosphido cluster $Mn_2Fe(\mu\text{-}H)(\mu\text{-}PPhCH_2PPh_2)(CO)_{10}$ (4) is formed in high yield.

The structure of compound 4 has been confirmed by X-ray diffraction, and the molecular structure is shown in Figure 2. The molecule contains an asymmetrical Mn_2Fe triangular core triply bridged by the phosphido–phosphine ligand $PPhCH_2PPh_2$, resulting from loss of a phenyl group in the former dppm ligand. This coordination mode is very similar to that found for the isoelectronic group 8 homonuclear metal clusters $Fe_3(\mu\text{-}H)(\mu\text{-}{}^iPrPCH_2P^iPr_2)(CO)_9$[17] and $Ru_3(\mu\text{-}H)(\mu\text{-}PhPCH_2PPh_2)](CO)_9$.[18] These clusters, however, required moderate thermal activation (ca. 70 °C) to be formed from the corresponding diphosphine-bridged precursors.[17,18] The phosphido-bridged edge (Fe(1)–Mn(2)) is also bridged by a hydrido ligand. The metal–phosphorus distances (Table IV) are not unusual, the ones involving the strongly bound phosphido group (P(1)) being predictably ca. 0.1 Å shorter than that corresponding to the phosphine group. However, Fe(1)–P(1) is very similar to Mn(2)–P(1) (2.2248 (8) and 2.2382 (8) Å, respectively). Considering the smaller covalent radius of Fe, this might be indicative of a somewhat stronger binding of the phosphido ligand to the manganese atom, perhaps compensated by a stronger binding of the hydrido ligand to iron. In fact, the Fe–H separation is smaller than the Mn(2)–H one, but the difference is only 4σ and is probably not really significant. The coordination sphere around the metals in 4 is completed with 10 CO ligands, three for each Fe and Mn(2) and four around Mn(1). Ignoring the intermetallic interactions, the environment around each metal is octahedral with one vacant position. The latter is occupied, in the case of Fe and Mn(2), by the corresponding bonds to Mn(1) (C(2)–Fe–Mn(1) = 158.3 (1)° and C(9)–Mn(2)–Mn(1) = 158.7 (1)°). The sixth coordination position for Mn(1) points roughly to the midway point of the Fe–Mn(2) vector. In addition, one of the carbonyls bonded to Mn(1) (C(7)–O(7)) has a semibridging character. This is indicated by a significant deviation from linearity (Mn(1)–C(7)–O(7) = 160.0 (3)°) and a relatively short contact distance with the second manganese atom of the molecule (C(7)···Mn(2) = 2.521 (3) Å). The latter is within the range of values reported for semibridging carbonyl ligands in several dimanganese complexes (ca. 2.33–2.61

Table IV. Selected Bond Lengths (Å) and Bond Angles (deg) for Compound 4

Fe(1)–Mn(1)	2.9065 (5)	Mn(1)–Mn(2)	2.8917 (6)
Fe(1)–Mn(2)	2.7247 (5)	Mn(1)–P(2)	2.3355 (8)
Fe(1)–P(1)	2.2248 (8)	Mn(1)–C(4)	1.846 (3)
Fe(1)–C(1)	1.825 (3)	Mn(1)–C(5)	1.854 (3)
Fe(1)–C(2)	1.785 (3)	Mn(1)–C(6)	1.803 (3)
Fe(1)–C(3)	1.788 (3)	Mn(1)–C(7)	1.871 (3)
Fe(1)–H(1)	1.56 (4)	Mn(2)–H(1)	1.77 (4)
Mn(2)–P(1)	2.2382 (8)	Mn(2)–C(9)	1.793 (3)
Mn(2)–C(8)	1.821 (3)	Mn(2)–C(10)	1.796 (3)
Fe(1)–C(5)	2.799 (3)	Mn(2)–C(7)	2.521 (3)
P(1)–C(11)	1.838 (3)	P(2)–C(11)	1.828 (3)
P(1)–C(20)	1.828 (3)	P(2)–C(30)	1.825 (3)
P(2)–C(40)	1.829 (3)		
C(1)–O(1)	1.132 (4)	C(6)–O(6)	1.136 (4)
C(2)–O(2)	1.132 (4)	C(7)–O(7)	1.153 (4)
C(3)–O(3)	1.134 (4)	C(8)–O(8)	1.136 (4)
C(4)–O(4)	1.132 (4)	C(9)–O(9)	1.145 (4)
C(5)–O(5)	1.138 (4)	C(10)–O(10)	1.144 (4)

Mn(2)–Fe(1)–Mn(1)	61.70 (1)	C(2)–Fe(1)–P(1)	96.3 (1)
P(1)–Fe(1)–Mn(1)	78.23 (2)	C(2)–Fe(1)–C(1)	91.5 (1)
P(1)–Fe(1)–Mn(2)	52.60 (2)	C(3)–Fe(1)–Mn(1)	105.6 (1)
C(1)–Fe(1)–Mn(1)	90.79 (9)	C(3)–Fe(1)–Mn(2)	142.4 (1)
C(1)–Fe(1)–Mn(2)	116.3 (1)	C(3)–Fe(1)–P(1)	91.2 (1)
C(1)–Fe(1)–P(1)	167.2 (1)	C(3)–Fe(1)–C(1)	98.1 (1)
C(2)–Fe(1)–Mn(1)	158.3 (1)	C(3)–Fe(1)–C(2)	95.4 (1)
C(2)–Fe(1)–Mn(2)	98.2 (1)	C(6)–Mn(1)–Fe(1)	158.8 (1)
Mn(2)–Mn(1)–Fe(1)	56.06 (1)	C(6)–Mn(1)–Mn(2)	144.3 (1)
P(2)–Mn(1)–Fe(1)	94.26 (2)	C(6)–Mn(1)–P(2)	91.7 (1)
P(2)–Mn(1)–Mn(2)	90.59 (2)	C(6)–Mn(1)–C(4)	90.0 (1)
C(4)–Mn(1)–Fe(1)	84.54 (9)	C(6)–Mn(1)–C(5)	91.8 (1)
C(4)–Mn(1)–Mn(2)	87.4 (1)	C(7)–Mn(1)–Fe(1)	115.4 (1)
C(4)–Mn(1)–P(2)	177.9 (1)	C(7)–Mn(1)–Mn(2)	59.4 (1)
C(5)–Mn(1)–Fe(1)	67.9 (1)	C(7)–Mn(1)–P(2)	88.90 (9)
C(5)–Mn(1)–Mn(2)	123.9 (1)	C(7)–Mn(1)–C(4)	90.1 (1)
C(5)–Mn(1)–P(2)	90.06 (9)	C(7)–Mn(1)–C(5)	176.6 (1)
C(5)–Mn(1)–C(4)	91.0 (1)	C(7)–Mn(1)–C(6)	85.0 (1)
Mn(1)–Mn(2)–Fe(1)	62.25 (1)	C(9)–Mn(2)–P(1)	90.2 (1)
P(1)–Mn(2)–Fe(1)	52.15 (2)	C(9)–Mn(2)–C(8)	91.5 (1)
P(1)–Mn(2)–Mn(1)	78.36 (2)	C(10)–Mn(2)–Fe(1)	150.6 (1)
C(8)–Mn(2)–Fe(1)	113.01 (9)	C(10)–Mn(2)–Mn(1)	111.4 (1)
C(8)–Mn(2)–Mn(1)	95.1 (1)	C(10)–Mn(2)–P(1)	99.0 (1)
C(8)–Mn(2)–P(1)	165.16 (9)	C(10)–Mn(2)–C(8)	95.8 (1)
C(9)–Mn(2)–Mn(1)	158.7 (1)	C(9)–Mn(2)–C(10)	88.0 (1)
Mn(2)–P(1)–Fe(1)	75.25 (3)	C(11)–P(2)–Mn(1)	110.2 (1)
C(11)–P(1)–Fe(1)	114.8 (1)	C(30)–P(2)–Mn(1)	114.1 (1)
C(11)–P(1)–Mn(2)	124.9 (1)	C(30)–P(2)–C(11)	105.1 (1)
C(20)–P(1)–Fe(1)	121.6 (1)	C(40)–P(2)–Mn(1)	120.9 (1)
C(20)–P(1)–Mn(2)	117.62 (9)	C(40)–P(2)–C(11)	104.0 (1)
C(20)–P(1)–C(11)	102.5 (1)	C(40)–P(2)–C(30)	100.9 (1)
O(1)–C(1)–Fe(1)	178.2 (3)	O(6)–C(6)–Mn(1)	176.5 (3)
O(2)–C(2)–Fe(1)	178.2 (3)	O(7)–C(7)–Mn(1)	160.0 (3)
O(3)–C(3)–Fe(1)	177.9 (3)	O(8)–C(8)–Mn(2)	177.9 (3)
O(4)–C(4)–Mn(1)	177.9 (3)	O(9)–C(9)–Mn(2)	178.8 (3)
O(5)–C(5)–Mn(1)	169.7 (3)	O(10)–C(10)–Mn(2)	174.7 (3)
P(2)–C(11)–P(1)	106.9 (1)	Mn(2)–H(1)–Fe(1)	109.8 (22)

Table V. Mn–Fe Single-Bond Lengths (Å) in Heterometallic Species Related to Compound 4

compd	[Mn–Fe]	ref
$Cp(CO)_2FeMn(CO)_5$	2.848 (4)	21a
$(\mu\text{-}AsMe_2)(CO)_4FeMn(CO)_4$	2.825 (5)	21b
$(\mu\text{-}PPh_2)(CO)_4FeMn(CO)_4$	2.760 (4)	21c
$(\mu\text{-}C{=}CHPh)(CO)_3FeMnCp(CO)_2$	2.742 (4)	21d
$\mu\text{-}PPh\{(CO)_6Fe_2MnCp(\mu\text{-}CO)_2\}$	2.747 (4)[a]	21e

---

[17] Brauer, D. J.; Hietkamp, S.; Sommer, H.; Stelzer, O. *Angew. Chem., Int. Ed. Engl.* 1984, *23*, 734.

[18] Lugan, N.; Bonnet, J. J.; Ibers, J. A. *J. Am. Chem. Soc.* 1985, *107*, 4484.

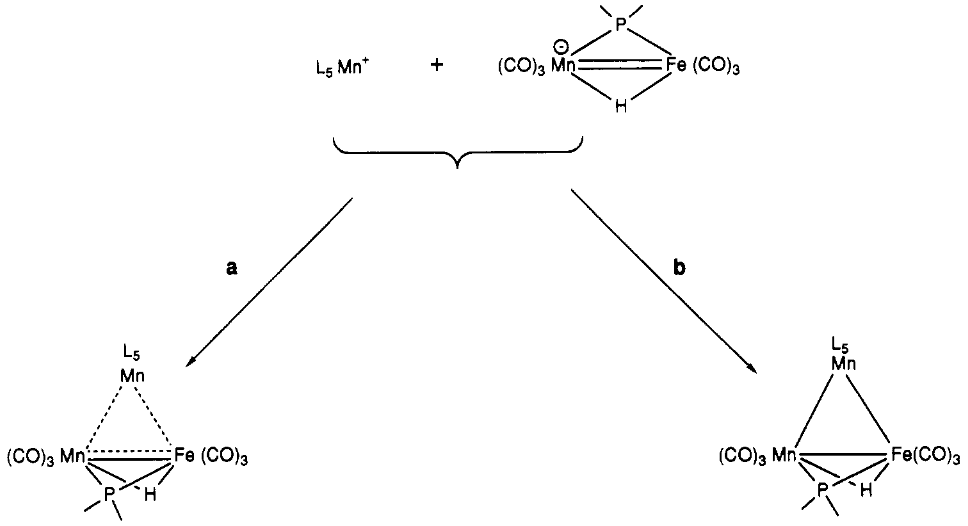

Figure 3. Fragment approach to the bonding in compound 4: (a) $L_5Mn^+ \leftrightarrow CH_3^+$; (b) $L_5Mn^+ \leftrightarrow CH_2$ (see text).

Å).[19a-e] Furthermore, the "asymmetry parameter"[19f] for the Mn(1)–C(7)···Mn(2) interaction is 0.35, well within the range of values (0.1–0.6) attributed to semibridging carbonyls.[19f]

Compound 4 is a 48e cluster species and, therefore, electron precise. As a result, the intermetallic separations can be expected to be in the range of the single metal–metal bonds. This is the case for the Mn(1)–Mn(2) length, 2.8917 (6) Å, very close to the value found for $Mn_2(CO)_{10}$ (2.9038 (6) Å).[20] As for the manganese–iron lengths, the Mn(1)–Fe distance, 2.9065 (5) Å, is somewhat longer than those found in related Fe–Mn singly bonded compounds (ca. 2.74–2.85 Å;[21a-e] Table V), whereas the phosphido-bridged distance, 2.7247 (5) Å, is slightly shorter, even when compared with the phosphido-bridged species $(CO)_4Fe(\mu\text{-}PPh_2)Mn(CO)_4$ (2.760 (4) Å).[21c] There might be electronic effects behind these small deviations. In fact, a normal electron count on this 48e cluster would leave 18e around Fe but 19 around Mn(1) and 17 around Mn(2). We can overcome this asymmetric distribution by assuming a formal oxidation state of 1+ at Mn(1) and 1− at Mn(2). This leads us to an interesting bonding picture of 4, where the metal triangle is the result of the interaction of a d^6 ML_5 fragment (Mn(1)) and the unsaturated dimetal moiety $(CO)_3Fe(\mu\text{-}H)(\mu\text{-}P)Mn(CO)_3^-$ (Mn=Fe) (P = $PPhCH_2PPh_2$; Figure 3). As previously stated, a d^6 ML_5 fragment (derived from an octahedron) can be considered isolobal with either CH_3^+ or CH_2. In the first case, interaction between fragments is restricted to a 3c–2e bond, and we would expect an Fe–Mn(2) distance significantly shorter than that corresponding to a single bond, whereas Mn(1)–Mn(2) and Mn(1)–Fe distances should be longer ((a) in Figure 3). On the other hand, if MnL_5^+ behaves like CH_2, there will be four electrons for the interaction between fragments, and single metal–metal bonds can be expected (the metallacyclopropane extreme, (b) in Figure 3). Of course, for a particular compound, any intermediate situation is possible, but considering the intermetallic distances in 4, essentially consistent with the presence of single metal–metal bonds as discussed above, we can conclude that 4 is much closer to the second extreme approach. Finally, the presence of a semibridging carbonyl at Mn(1) is consistent with the artificial charge separation introduced at the manganese atoms, as this would partially relieve the excess of charge at Mn(2) through a $d\pi(Mn)\text{–}\pi^*(CO)$ interaction.[22]

Spectroscopic data for 4 in solution (Table I) are entirely consistent with its solid-state structure and will not be discussed in detail. The relevant data are the hydrido resonance (δ −15.18 ppm) exhibiting P–H coupling with the phosphido ligand in the range found for bis-octahedral $Mn_2(\mu\text{-}H)(\mu\text{-}PRR')(CO)_6(\mu\text{-}L_2)$ complexes (L_2 = dppm, tedip; R, R′ = H, Cy, Ph)[8a] and a highly deshielded ^{31}P resonance (157.2 ppm), indicative of a phosphido ligand across a metal–metal bond.[23] The positioning of this ligand between Mn and Fe atoms in solution is suggested by the significantly smaller width of its resonance ($w_{1/2}$ = 33 Hz), when compared with that for the 39.8 ppm resonance (66 Hz, $Mn\text{–}PPh_2\text{–}CH_2\text{–}$).

Reactions of Dihydrides 1 and 2 with $M(CO)_6$ (M = Cr, Mo, W). Compound 1 does not react to any appreciable extent with the group 6 metal hexacarbonyls at room temperature or under moderate heating. However, under photochemical conditions some reactions occur, the result being strongly dependent on the nature of the group 6 metal. In the case of chromium, a slow decomposition reaction occurs at −30 °C, leading to the formation of the previously known $Mn_2(\mu\text{-}tedip)(CO)_8$.[24] The case of molybdenum is intermediate and will be discussed later. Finally, UV irradiation of an equimolecular mixture of 1 and $W(CO)_6$ in petroleum ether at −10 °C gives the dark purple cluster $Mn_2W(\mu\text{-}H)_2(\mu\text{-}tedip)(CO)_{11}$ (5) in essentially quantitative yield.

Compound 5 is unstable in solution above −10 °C, decomposing to the starting materials 1 and $W(CO)_6$. Be-

---

(19) (a) Keijsker, J.; Van Koten, G.; Vrieze, K.; Zoutberg, M.; Stam, C. H. *Organometallics* **1985**, *4*, 1306. (b) Ferguson, G.; Laws, W. J.; Parvez, M.; Puddephatt, R. J. *Organometallics* **1983**, *2*, 276. (c) Williams, G. D.; Geoffroy, G. L.; Rheingold, A. L. *Organometallics* **1986**, *5*, 894. (d) Schauer, D. F.; Schriver, D. F. *Angew. Chem., Int. Ed. Engl.* **1987**, *26*, 225. (e) Fong, R. H.; Hersh, W. H. *J. Am. Chem. Soc.* **1987**, *109*, 2843. (f) Curtis, M. D.; Han, K. R.; Butter, W. M. *Inorg. Chem.* **1979**, *19*, 2096.

(20) Churchill, M. R.; Amoh, K. N.; Wassermann, H. J. *Inorg. Chem.* **1981**, *20*, 1609.

(21) (a) Hansen, R. J.; Jacobson, R. A. *J. Organomet. Chem.* **1966**, *6*, 389. (b) Vahrenkamp, H. *Chem. Ber.* **1973**, *106*, 2570. (c) Vahrenkamp, H. *Z. Naturforsch., B: Anorg. Chem. Org. Chem.* **1975**, *30B*, 814. (d) Andrianov, V. G.; Struchdov, Y. T.; Kolonbonc, N. E.; Antonouc, A. B.; Obezyu, M. S. *J. Organomet. Chem.* **1976**, *122*, C33. (e) Huttner, G.; Frank, A.; Mohr, G. *Z. Naturforsch., B: Anorg. Chem. Org. Chem.* **1976**, *31B*, 1161. (f) Schauer, C. K.; Shriver, D. F. *Angew. Chem., Int. Ed. Engl.* **1987**, *26*, 225.

(22) Cotton, F. A.; Wilkinson, G. *Advanced Inorganic Chemistry*, 5th ed.; Wiley: New York, 1988; Chapter 22, p 1030.

(23) Carty, A. J.; Mclaughlin, S. A.; Nucciarane, D. In *Phosphorus-31 NMR Spectroscopy in Stereochemical Analysis*; Verkade, J. G., Quin, L. D., Eds.; VCH: Deerfield Beach, FL, 1987; Chapter 16.

(24) Riera, V.; Ruiz, M. A. *J. Chem. Soc., Dalton Trans.* **1986**, 2617.

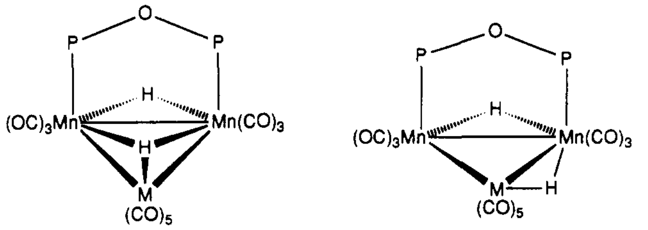

5 M=W

6a M=Mo

6b M=Mo

Figure 4. Proposed structures for compounds 5 and 6 (POP = $(EtO)_2POP(OEt)_2$).

cause of this, the IR spectra of **5** in solution (but not in the solid state) are always "contaminated" with absorptions corresponding to these species, and therefore the complete spectrum can not be unambiguously identified, due to possible accidental coincidences. Even so, the IR spectrum of **5** in petroleum ether exhibits a characteristic band of medium intensity at 2081 cm^{-1} (2079 cm^{-1} in Nujol emulsion), which is clearly indicative of the presence of a $W(CO)_5$ moiety in the molecule. The ^{31}P NMR spectrum contains just one singlet which remains unchanged (except for its progressive sharpening) down to −80 °C, with a chemical shift characteristic of the tedip ligand bridging metal–metal-bonded manganese atoms. The ^{1}H NMR spectrum shows two triplets of equal intensity for the methyl groups of the tedip ligand, indicative of different chemical environments at either side of the Mn_2POP pseudoplane. Additionally, the spectrum exhibits two distinct hydride resonances, which appear as triplets because of coupling with two equivalent phosphorus atoms. The triplets show a further 5-Hz splitting due to mutual $^{2}J(HH)$ coupling, as confirmed by double-resonance experiments. At 273 K, the high-field resonance shows ^{183}W satellite peaks, with relative intensities corresponding to a single tungsten atom. $J(WH)$ is 40 Hz, similar to the values found for other bridging hydrido ligands involving tungsten (for example, ca. 40–50 Hz for the complexes $(CO)_4LW(\mu\text{-}H)MPPh_3$ L = CO, $P(OMe)_3$; M = Au, Ag)[25] and $W_2(\mu\text{-}H)(\mu\text{-}L_2)(CO)_7(NO)$ (L_2 = diphosphine ligand).[26] Therefore, the high-field resonance (−24.0 ppm) is attributed to a μ_3-hydrido ligand bridging the tungsten and manganese atoms (Figure 4) and the −17.1 ppm resonance to a μ_2-hydrido ligand bridging both manganese atoms symmetrically. These assignments are further supported by the measured P–H coupling constants. The μ_2 ligand displays a $J(PH)$ value of 27 Hz, in the 29 ± 2 Hz range persistently found for $Mn_2(\mu_2\text{-}H)(\mu\text{-}tedip)$ complexes with H and tedip in a relative cis arrangement.[8a,15,27] The other hydrido ligand exhibits a $J(PH)$ value significantly lower (21 Hz), as can be expected from its μ_3 nature, which implies that less s-electron density is available for Mn–H bonding, compared to the case for a μ_2-hydrido ligand.

On the whole, the structure proposed for **5** (Figure 4) is closely related to that found for the complexes $Mn_2(\mu\text{-}H)_2(\mu\text{-}X)(\mu\text{-}dppm)(CO)_6$ (X = $AuPPh_3^+$, $Ag(OClO_3)PPh_3$),[7] if we allow X to be $W(CO)_5$. This suggests that the interaction between **1** and $W(CO)_5$ to give **5** is best described in terms of a weak acid–base interaction between a $Mn_2(\mu\text{-}H)$ bond in **1** (behaving as the base) and the $W(CO)_5$ fragment (behaving as the acid and therefore resembling $AuPPh_3^+$ or H^+). This contrasts strongly with the behavior shown by $Fe(CO)_4$ toward **1** (methylene-like). As will be discussed later on, the case of molybdenum seems to be intermediate between the above situations.

When a petroleum ether solution of compound **1** is exposed at −30 °C to UV light in the presence of $Mo(CO)_6$, no new compounds can be detected by room-temperature IR spectroscopy. However, NMR (−30 °C) monitoring of this reaction (carried out also at −30 °C and using CD_2Cl_2 as solvent) shows the presence of two new species in the reaction mixture, which are thought to be two isomers of the molybdenum dimanganese cluster $Mn_2Mo(\mu\text{-}H)_2(\mu\text{-}tedip)(CO)_{11}$ (**6a,b**). These new species could not be isolated through either crystallization of the reaction mixture (petroleum ether solution) at −20 °C or chromatography on alumina at −40 °C. The latter yielded only fractions containing $Mo(CO)_6$ and compound **1**. The overall amount of **6a** + **6b** relative to **1** in the reaction mixtures analyzed never reached more than ca. 15%, as determined by ^{1}H NMR. In fact, after long irradiation periods, the only hydrido-containing species present in the solution was the starting material **1**. This can be explained by assuming for **6** a thermal decomposition at −30 °C (perhaps superimposed with some photochemical decomposition) similar to that observed for **5** at room temperature.

Compound **6a** displays ^{1}H and ^{31}P NMR features very similar to those found for **5** (Table I) and, accordingly, is thought to be the molybdenum analogue of **5** (Figure 4). In contrast with this, **6b** has a less symmetrical structure, denoted in the ^{31}P spectrum by a broad doublet at 173.4 ppm ($J(PP)$ = 50 Hz). We have not been able to locate its "partner" resonance, which is probably obscured by the very strong and relatively broad resonance of **1** always present in the solutions analyzed. In any case, this means that the phosphorus atoms of the tedip ligand have distinct chemical environments in the molecule. In agreement with this, the ^{1}H NMR spectrum of **6b** shows the presence of two different hydrido ligands, appearing in the form of a doublet (−14.5 ppm, $J(PH)$ = 44 Hz) and a triplet (−24.1 ppm, $J(PH)$ = 29 Hz), respectively. The chemical shift and phosphorus coupling of the latter allows the assignment of this resonance to a hydrido ligand bridging two manganese atoms cis to the tedip bridge. Finally, the low-field resonance is attributed to a bridging hydride between Mn and Mo atoms (Figure 4), in accordance with its multiplicity and lower chemical shift. From a structural point of view, then, $Mo(CO)_5$ seems to be able to display both possible behaviors for a d^6 ML_5 fragment, i.e., either a CH_3^+-like one (complex **6a**), as was the case for $W(CO)_5$, or a CH_2-like one (complex **6b**), as found for $Fe(CO)_4$. This is an indication of the subtleness of the factors governing the overall chemical behavior of these 16-electron species.

When reactions analogous to those just described for **1** and $M(CO)_6$ (M = Cr, Mo, W) were carried out using the dppm-bridged dihydride **2**, no new species were detected. This is not to be expected on electronic grounds alone, as dihydride **2** is a better electron-donor molecule than **1**.[7] Therefore, it seems likely that steric repulsions between the bulky dppm ligand (when compared with tedip) and the incoming $M(CO)_5$ fragment are the main factors that preclude the formation of reasonably stable dppm analogues of compounds **5** and **6**.

Experimental Section

General Procedures. All reactions were carried out under a nitrogen atmosphere using standard Schlenk techniques.

---

[25] Green, M.; Orpen, A. G.; Salter, I. D.; Stone, F. G. A. *J. Chem. Soc., Dalton Trans.* **1984**, 2497.

[26] Lin, J. T.; Chang, K. Y.; Wang, S. Y.; Wen, Y. S.; Tseng, L. H.; Chang, C. C.; Peng, S. M.; Wang, Y.; Lee, G. H. *Organometallics* **1991**, *10*, 2377.

[27] Riera, V.; Ruiz, M. A.; Tiripicchio, A.; Tiripicchio-Camellini, M. *J. Chem. Soc., Dalton Trans.* **1987**, 1551.

Photochemical reactions were performed by irradiation with an Applied Photophysics 400-W mercury lamp using jacketed Pyrex vessels refrigerated by a closed 2-propanol circuit kept at the desired temperature with a Haake F-3 cryogenerator. Solvents were purified according to standard literature procedures[28] and distilled under nitrogen prior to use. Petroleum ether refers to the fraction distilling in the range 60–65 °C. $M(CO)_6$ (M = Cr, Mo, W) were purchased from commercial suppliers and used as received. Bis(diphenylphosphino)methane,[29] $Mn_2(\mu\text{-}H)_2(CO)_6(\mu\text{-dppm})$,[6b] $Mn_2(\mu\text{-}H)_2(CO)_6(\mu\text{-tedip})$,[5] and $Fe_2(CO)_9$[30] were prepared by literature methods. Alumina for column chromatography was deactivated by appropriate addition of water under nitrogen to the commercial material (Aldrich, neutral, activity I). Infrared spectra were recorded on a Perkin-Elmer 1720-X FT spectrometer. NMR spectra were recorded on a Bruker AC 300 spectrometer at 300.13 MHz (^1H) and 121.5 MHz (^{31}P). Chemical shifts are referred to internal TMS (^1H) or external 85% H_3PO_4 aqueous solution. Elemental C and H analyses were obtained with a Perkin-Elmer 204B microanalyzer.

Preparation of $Mn_2Fe(\mu\text{-}H)_2(\mu\text{-tedip})(CO)_{10}$ (3). Solid $Fe_2(CO)_9$ (0.034 g, 0.093 mmol) was added to a solution of 1 (0.050 g, 0.093 mmol) in toluene (10 mL), and the mixture was stirred in the dark for 2 h at room temperature, affording a red-violet solution. The solution was concentrated under vacuum to ca. 1 mL and chromatographed on an alumina column at −30 °C (activity IV, 20 × 2.5 cm) prepared in petroleum ether. Elution with petroleum ether and CH_2Cl_2–petroleum ether (1:25) gave two yellow fractions and one orange fraction, respectively, containing trace amounts of unidentified species. Elution with CH_2Cl_2–petroleum ether (1:19) gave one dark red fraction which yielded, after removal of solvent under vacuum, compound **3** as a dark red microcrystalline powder (0.042 g, 60%). ν(CO) (petroleum ether): 2081 m, 2033 vs, 2007 vs, 1984 s, 1978 m, sh, 1969 m, 1954 w cm^{-1}. Anal. Calcd for $C_{18}H_{22}FeMn_2O_{15}P_2$ (**3**): C, 30.6; H, 3.1. Found: C, 31.0; H, 3.2.

Preparation of $Mn_2Fe(\mu\text{-}H)(\mu\text{-}Ph_2PCH_2PPh)(CO)_{10}$ (4). Solid $Fe_2(CO)_9$ (0.027 g, 0.075 mmol) was added to a solution of **2** (0.050 g, 0.075 mmol) in toluene (10 mL), and the mixture was stirred in the dark for 2 h at room temperature. The mixture was chromatographed at −30 °C as described for **3**. Elution with petroleum ether–CH_2Cl_2 (4:1) gave a deep red fraction which yielded, after removal of solvent under vacuum, compound **4** as a dark red microcrystalline powder (0.045 g, 79%). Further elution with dichloromethane gave a yellow fraction containing trace amounts of unidentified species. The crystals used in the X-ray diffraction study were grown by slow diffusion between a concentrated dichloromethane solution of **4** and petroleum ether, at room temperature. ν(CO) (toluene): 2066 m, 2021 vs, 2011 s, 1980 m, 1962 m, 1948 m, sh, 1937 m, 1902 w cm^{-1}. Anal. Calcd for $C_{29}H_{18}FeMn_2O_{10}P_2$ (**4**): C, 50.9; H, 2.4. Found: C, 51.2; H, 2.5.

Preparation of $Mn_2W(\mu\text{-}H)_2(\mu\text{-tedip})(CO)_{11}$ (5). A solution of compound 1 (0.050 g, 0.093 mmol) and $W(CO)_6$ (0.033 g, 0.093 mmol) in petroleum ether (10 mL) was irradiated with visible–UV light for 1 h at −10 °C. The solution was then filtered through diatomaceous earth at the same temperature. Removal of the solvent under vacuum yielded compound **5** (0.068 g, 85%) as a dark purple microcrystalline powder. Complex **5** is thermally unstable at room temperature in solution but can be safely handled in the solid state without noticeable decomposition. It can be recrystallized from petroleum ether at −20 °C. ν(CO) (petroleum ether): 2081 m, 2037 s, 2025 s, 1991 w, 1972 s, 1947 sh, vs, 1942 vs, 1919 w cm^{-1}. ν(CO) (Nujol emulsion): 2079 s, 2030 vs, 2016 vs, 1996 s, 1977 vs, 1946 vs, br, 1933 vs, br cm^{-1}. Anal. Calcd for $C_{19}H_{22}Mn_2O_{16}P_2W$ (**5**): C, 26.4; H, 2.6. Found: C, 26.1; H, 2.9.

Crystal Structure Analysis of Compound 4. Details of the data collection and refinements are given in Table II. All calculations were carried out with the program CRYSTALS.[31] No absorption correction on the measured reflections was necessary, as suggested by a flat ψ scan. The structure was solved by direct methods and subsequent Fourier maps. Least-squares refinements were carried out in two blocks. Hydrogen atoms were found on difference maps, except for two phenyl protons, which were geometrically positioned. They were refined and given an isotropic overall thermal parameter. Atoms were corrected for anomalous dispersion. A secondary extinction correction was applied. The final positional and thermal parameters for non-hydrogen atoms and the hydrido ligand are listed in Table III. Selected bond lengths and angles are given in Table IV. Figure 2 is an ORTEP drawing of the molecule with the numbering scheme (C(phenyl) labels omitted for clarity). Thermal ellipsoids are drawn at 30% probability.

Acknowledgment. We thank the Ministerio de Educación y Ciencia of Spain for a grant (to R.C.) and the DGICYT of Spain for financial support (Project PB88-0467).

Supplementary Material Available: A drawing of the molecular structure of compound 4 showing the numbering scheme for all atoms and tables of atomic coordinates and thermal parameters for hydrogen atoms, anisotropic thermal parameters, and additional bond lengths and angles (4 pages). Ordering information is given on any current masthead page.

OM920256G

---

[28] Perrin, D. D.; Armarego, W. L. J.; Perrin, D. R. *Purification of Laboratory Chemicals*, 2nd ed.; Pergamon Press: Oxford, U.K., 1980.

[29] Aguiar, A. M.; Beisler, J. J. *Org. Chem.* **1964**, *29*, 1660.

[30] Braye, E. H.; Hübel, W. *Inorg. Synth.* **1966**, *8*, 178.

[31] Carruthers, J. R.; Watkin, D. W. CRYSTALS, an Advanced Crystallographic Computer Program; Chemical Crystallography Laboratory, Oxford University: Oxford, U.K., 1985.